ENDOCRINE SOCIETY

A new multi-system disorder caused by the Gαs mutation p.F376V

Heike Biebermann, Gunnar Kleinau, Dirk Schnabel, Detlef Bockenhauer, Louise C. Wilson, Ian Tully, Sarah Kiff, Patrick Scheerer, Monica Reyes, Sarah Paisdzior, John W. Gregory, Jeremy Allgrove, Heiko Krude, Michael Mannstadt, Thomas J. Gardella, Mehul Dattani, Harald Jüppner, Annette Grüters

Advance Articles are PDF versions of manuscripts that have been peer reviewed and accepted but not yet copyedited. The manuscripts are published online as soon as possible after acceptance and before the copyedited, typeset articles are published. They are posted "as is" (i.e., as submitted by the authors at the modification stage), and do not reflect editorial changes. No corrections/changes to the PDF manuscripts are accepted. Accordingly, there likely will be differences between the Advance Article manuscripts and the final, typeset articles. The manuscripts remain listed on the Advance Article page until the final, typeset articles are posted. At that point, the manuscripts are removed from the Advance Article page.

DISCLAIMER: These manuscripts are provided "as is" without warranty of any kind, either express or particular purpose, or non-infringement. Changes will be made to these manuscripts before publication. Review and/or use or reliance on these materials is at the discretion and risk of the reader/user. In no event shall the Endocrine Society be liable for damages of any kind arising references to, products or publications do not imply endorsement of that product or publication.

ENDOCRINE SOCIETY

A new multi-system disorder caused by the Gαs mutation p.F376V

Heike Biebermann [1,§], Gunnar Kleinau [1,2,§], Dirk Schnabel [3,4,§], Detlef Bockenhauer [5], Louise C. Wilson [6], Ian Tully [7], Sarah Kiff [8], Patrick Scheerer [2], Monica Reyes [9], Sarah Paisdzior [1], John W. Gregory [10], Jeremy Allgrove [8], Heiko Krude [1], Michael Mannstadt [9], Thomas J. Gardella [9], Mehul Dattani [8,11,#], Harald Jüppner [9,#], Annette Grüters [3,9,12,#,*]

corresponding author

[1-4] *Charité – Universitätsmedizin Berlin, corporate member of Freie Universität Berlin, Humboldt-Universität zu Berlin, Germany;*

[1] *Institute of Experimental Pediatric Endocrinology, Augustenburger Platz 1, 13353 Berlin, Germany;*

[2] *Institut für Medizinische Physik und Biophysik, Group Protein X-ray Crystallography and Signal Transduction; 10117 Berlin, Germany;*

[3] *Department for Pediatric Endocrinology and Diabetology; 13353 Berlin, Germany;*

[4] *Center for Chronically Sick Children, 13353 Berlin, Germany;*

[5] *UCL Centre for Nephrology, NW3 2PF London, UK; and Great Ormond Street Hospital for Children, Renal Unit, WC1N 3JH London, UK*

[6] *Department of Clinical Genetics, Great Ormond Street Hospital for Children, WC1N 3JH London, UK;*

[7] *Department of Clinical Genetics, University Hospital of Wales, CF14 4XW Cardiff, UK;*

[8] *Department of Pediatric Endocrinology, Great Ormond Street Hospital for Children, WC1N 3JH London, UK;*

[9] *Endocrine Unit Massachusetts General Hospital and Harvard Medical School, 02114 Boston, Ma, USA;*

[10] *Division of Population Medicine, School of Medicine, CF14 4XN Cardiff University, UK;*

[11] *Section of Genetics and Epigenetics in Health and Disease, Genetics and Genomic Medicine Programme, UCL GOS Institute of Child Health, WC1N 1EH London, UK;*

[12] *University Hospital Heidelberg, 69120 Heidelberg, Germany*

ORCiD numbers:

0000-0003-2131-671X

Kleinau

Gunnar

Context: The alpha-subunit of the stimulatory G-protein (Gαs) links numerous receptors to adenylyl cyclase. Gαs, encoded by *GNAS,* is expressed predominantly from the maternal allele in certain tissues. Thus, maternal heterozygous loss-of-function mutations cause hormonal resistance, as in pseudohypoparathyroidism type Ia, while somatic gain-of-function mutations cause hormone-independent endocrine stimulation, as in *McCune-Albright Syndrome*.
Objective: We here report two unrelated boys presenting with a new combination of clinical findings that suggest both gain and loss of Gαs function.

Design, Setting: Clinical features were studied and sequencing of *GNAS* was performed. Signaling capacities of wild-type and mutant-Gαs were determined in the presence of different G protein-coupled receptors (GPCRs) under basal and agonist-stimulated conditions.

Results: Both unrelated patients presented with unexplained hyponatremia in infancy, followed by severe early-onset gonadotrophin-independent precocious puberty and skeletal abnormalities. An identical heterozygous *de novo* variant (c.1136T>G; p.F376V) was found on the maternal *GNAS* allele, in both patients; this resulted in a clinical phenotype that differ from known Gαs-related diseases and suggested gain-of-function at the receptors for vasopressin (V2R) and lutropin (LHCGR), yet increased serum parathyroid hormone (PTH) concentrations indicative of impaired proximal tubular PTH1 receptor (PTH1R) function. *In vitro* studies demonstrated that Gαs-F376V enhanced ligand-independent signaling at the PTH1R, LHCGR and V2R and, at the same time, blunted ligand-dependent responses. Structural homology modeling suggested mutation-induced modifications at the C-terminal α5-helix of Gαs that are relevant for interaction with GPCRs and signal transduction.

Conclusions: The Gαs p.F376V mutation causes a previously unrecognized multi-system disorder.

This study describes a multi-system disorder caused by a new heterozygous human Gαs mutation that induces both gain- and loss-of function effects in interplay with diverse G-protein coupled receptors.

Introduction

Heterotrimeric G-proteins, comprised of a specific alpha (α) subunit and associated beta (β) and gamma (γ) subunits, activate a variety of distinct intracellular signaling pathways (1,2). These signaling events are normally initiated when the G-protein heterotrimer interacts with the cytoplasmic portion of an agonist-activated G-protein-coupled receptor (GPCR) (3). Activating mutations in either a GPCR or a G-protein that increase ligand-independent signaling are the cause of several diseases (4,5).

The α-subunit of the stimulatory G-protein (Gαs), encoded by *GNAS* exons 1-13, links a large number of different GPCRs to the adenylyl cyclase/cAMP pathway. Through as-yet unknown mechanisms, Gαs expression from the paternal *GNAS* allele is reduced in a tissue-specific manner, such that cells of the renal proximal tubule, thyroid, pituitary, and several other tissues express Gαs predominantly from the maternal allele. Consequently inactivating Gαs mutations on the maternal allele, as in pseudohypoparathyroidism type Ia (PHP1A), lead to a multi-system disorder characterized by parathyroid hormone (PTH)-resistant hypocalcemia, impaired signaling at the thyrotropin receptor leading to reduced thyroid hormone production, and several other endocrine and developmental abnormalities (6).

Somatic gain-of-function mutations in Gαs that occur at either position R201 or R227 (7) are found in a variety of human cancers and benign endocrine tumors (8). In addition, mosaic expression of Gαs mutations at residue R201 give rise to the *McCune-Albright Syndrome*. Depending on the embryonic stage at which the somatic nucleotide change occurred, these patients present with a combination of different clinical and laboratory findings that can include gonadotropin-independent precocious puberty in early infancy that is resistant to treatment with GnRH agonists, hyperthyroidism, café-au-lait spots, and variable skeletal findings (9,10). R201-Gαs mutations are not transmitted through the germline, presumably because of early lethality due to excessive cAMP signaling (11).

Previously, two male patients with gonadotropin-independent precocious puberty and PTH-resistant hypocalcemia were shown to carry an identical Gαs mutation, A366S, which was

associated with agonist-independent activation of some GPCRs, yet hormonal resistance at others (12). Thus, these patients presented with LH-independent precocious puberty and resistance at the receptors for PTH (PTH1R) and thyrotropin (TSHR). These discrepant findings were thought to be explained by instability of the Gαs mutant at body temperature, combined with agonist-independent activation of the lutropin receptor (LHCGR) because of accelerated release of GDP at the lower temperature of the testes.

We now report two unrelated male patients, who were referred to us with an unexplained combination of severe asymptomatic infantile hyponatremia, skeletal and growth plate abnormalities, early-onset pubertal development and apparent PTH-resistance in the proximal, but not in the distal renal tubules. The same novel Gαs mutation (p.F376V) was identified in both boys and *in vitro* studies revealed GPCR-specific signaling abnormalities, which explained the patients unusual phenotypes, i.e. symptoms that suggested both gain- and loss-of function.

Patients and Methods

The parents of both patients have consented to the reported investigations. Two unrelated boys presented first with unexplained hyponatremia in infancy and subsequently with early-onset gonadotrophin-independent precocious puberty, elevated serum PTH concentrations and unique skeletal abnormalities. This previously unreported combination of symptoms and laboratory findings was indicative of both gain- and loss-of-function at different GPCRs that had not been encountered in other Gαs-related diseases (clinical data are summarized in Table 1, comparative phenotypic information is provided in Table 2, and detailed patient information are available in the supplementary material).

DNA sequence analyses
GNAS exons 1-13 underwent direct nucleotide sequence analysis for patients 1 and 2; whole exome sequencing was furthermore performed for patient 1. To determine the parental origin of the mutation, a PCR fragment was amplified from both patients and their parents that extends from intron 6 to the 3'-non-coding region telomeric of exon 13, i.e. the exon that comprises the patient`s mutation. The PCR products from each patient were cloned into a TA cloning vector (Life technologies, Darmstadt, Germany) and 10 independent colonies underwent nucleotide sequence analysis.

Construction of G-alpha variants
Wild-type (wt) human Gαs (NM_000516) was cloned into the pcDps expression vector, as described previously (13); investigated Gαs variants were introduced by standard mutagenesis technique. To determine if G-protein expression is modified in the presence of tested GPCRs, a luciferase (NanoLuc) was introduced between amino acids 324 and 325 of the wild-type and mutant Gαs.

Determination of WT-Gαs and Gαs-variant expression via luciferase activity
HEK293 cells lacking Gαs (GSG-5 cells) were seeded in white 96-well plates (1.5×10^4/well). The following day, cells were co-transfected with the NanoLuc-modified wild-type and mutant Gαs, in combination with the TSHR, LHCGR, MC4R, PTH1R, V2R, or empty vector using Metafectene® (Biontex, Munich, Germany) according to manufacturer's protocol using Opti-MEM without phenol red. 24h after transfection, 25 µl/well NanoLuc substrate Nano-Glo™ (50 µM) was injected using Berthold Mithras LB 940. The luciferase activity was measured at 460 nm ± 25nm in triplicates.

Determination of signaling properties of Gαs-variants

Functional characterization of wt and mutant Gαs was performed using mouse fibroblast 2B2 cells that lack *Gnas* exon 2 on both alleles (14) and GSG-5 cells, derived from the human embryonic kidney cell line (HEK293), which had been engineered by CRISPR-Cas9 to lack Gαs; the latter cells were stably transfected to express the luciferase-based GloSensor™ cAMP reporter. Cells were seeded in 96-well plates ($1x10^4$/well). Next day the different GPCRs (TSHR, MC4R, PTH1R, LHCGR or V2R) were co-transfected with wt or mutant Gαs at a ratio 1:1 using Metafektene (Biontex, Munich, Germany) for 2B2 cells or Lipofectamine-2000 (Invitrogen Promega) for GSG-5 cells according to the manufacturers' protocols. Two days later cAMP accumulation assays were performed at 37°C as previously described (15). For GSG-5 cells, intracellular cAMP was monitored by treating the cells with luciferin (5 mM) and measuring changes in luminescence over time at room temperature using a PerkinElmer Envision plate reader. Basal cAMP was measured for 14 minutes immediately following the addition of luciferin, and ligand-stimulated cAMP responses were subsequently measured for 88 minutes following the addition of PTH(1-34) (100 nM).

Data analysis

All data are given as raw data (mean ± SEM) obtained from four independent experiments performed in triplicates. Bar graphs and dose-response curves as well as statistical analyses were generated using GraphPad Prism Version 6.0 (GraphPad Software, San Diego, CA). Data obtained with GSG-5 cells are reported as means ± SEM of six independent assays; for each assay, data from replicate wells (twelve for basal and two for each PTH concentration) were averaged before combining the data to obtain the mean values for the six independent experiments.

Structural homology modeling

A structural homology model of Gαs in its inactive conformation was generated to study the interactions of F376 in the context of the wild-type protein. We compared the inactive model with the already known active and receptor-bound Gαs conformation (16). In brief, an inactive state structure of Gαs without the N-terminal helix is already available (PDB entry 1AZT (17)) as well as for the trimeric Gi protein (PDB entry 1GP2 (18)). To build a completed inactive Gαs model, the available Gαs crystal structure was superimposed onto the α-subunit of Gi and the N-terminal α1-helix (which has not yet been resolved for the Gαs structure) and was inserted by substituting the N-terminal helix of Gαi into the incomplete Gαs structure. The mutant amino acids were then introduced *in silico* into the chimeric template of wild-type Gαs. The resulting completed heterotrimeric Gαs model was refined by geometry optimization and energy minimization of the side chains until converging at a termination gradient of 0.2 kcal/mol*Å with constraint backbone atoms, which were finally released in a second minimization step until converging at a termination gradient of 0.1 kcal/mol*Å. The Gαs-variants (p.F376V, p.F376Y, and p.F376M) were introduced into the inactive wild-type Gαs model to unravel the potential local impact of these side chain variations. All structural modifications were performed using the software SYBYL-X 2.0 (Certara, NJ, US). The AMBER F99 force field was used for energy minimization. Structure images were produced using the PyMOL Molecular Graphics System, Version 1.5, Schrödinger, LLC.

Results

A previously unrecognized phenotype in two unrelated patients

Both male patients, 7 and 3.5 years of age at last follow-up, respectively, were born at term after uneventful pregnancies to unrelated parents with no family history of note. A more detailed patient description and discussion is provided in the supplemental material.

Nephrogenic syndrome of inappropriate anti-diuresis (NSIAD)
Both patients presented in the first few days of life with clinically asymptomatic hyponatremia in the absence of hyperkalemia, which was detected incidentally when analyzing blood glucose and gases. Investigations revealed no evidence for defects in mineralocorticoid production (hypoaldosteronism) or action (i.e. pseudohypoaldosteronism) and both patients were deemed euvolemic. A mutation in vasopressin receptor 2 (*AVPR2*; protein name V2R) causing NSIAD was suspected in patient 1 but excluded by direct nucleotide sequence analysis; treatment with sodium supplementation was started. In patient 2, hypertension induced by sodium supplements and mineralocorticoids (fludrocortisone) was treated with amlodipine. Copeptin, a marker of arginine vasopressin (AVP) secretion, also known as CT-proAVP, was low (<3.6 pmol/l) on four occasions when serum sodium was normal or low, yet urine osmolality remained persistently elevated (>800 mosm/kg). A tolvaptan (V2R antagonist) challenge failed to increase urine output and to decrease urine osmolality consistent with NSIAD. Treatment with sodium alone or with sodium and fludrocortisone were discontinued in both patients at 3 years of age.

PTH-resistance in the proximal, but not the distal, renal tubules
Both patients had persistently elevated PTH serum concentrations in association with total calcium concentrations that were within the normal range, and serum phosphate levels that were at the upper end of the normal range or slightly elevated. 25(OH)D and 1,25(OH)$_2$D concentrations were within the normal range. Both had a low urinary calcium/creatinine ratio (patient 1: 0.05 mol/mol, patient 2: 0.09 mol/mol) and there was no evidence of nephrocalcinosis. Treatment of patient 1 with calcitriol and of patient 2 with 1-alpha calcidol at relatively low doses reduced PTH serum concentrations.

Evidence for increased PTH1R activity in bone and growth plates
Both patients had enlarged and persistently open anterior fontanelles beyond the age of one year, rather short distal phalanges, and subtle widening of the growth plates, but neither had, until the age of 3 yrs, clinical or radiographic features of AHO such as brachymetacarpy, and there was no evidence for fibrous dysplasia. Patient 1 developed severe deformities of the lower limbs and suffered a spontaneous right tibial fracture at 1.5 years of age, which required surgery [Fig. 1]. At the age of 1.25 years, a skeletal survey of patient 2 showed subperiosteal erosions, particularly at the proximal radius, metacarpals and middle phalanges, and evidence of acro-osteolysis at the distal phalanges of hands and feet.

Gonadotrophin-independent precocious puberty
Both patients were noted to have symmetrical testicular enlargement and signs of precocious puberty at about 2 years of age that were associated with accelerated growth and significantly advanced bone age. Elevated serum testosterone concentrations were noted; yet there was no increase in luteinizing hormone (LH) and follitropin (FSH) secretion after challenge with gonadotropin-releasing hormone (GnRH), i.e. findings consistent with gonadotrophin-independent precocious puberty [Tab 1]. Treatment with an aromatase inhibitor (Anastrozole) and initially cyproterone acetate (anti-androgen) was therefore commenced in both patients; the latter medication was subsequently substituted by Bicalutamide. Based on the radiographic findings at follow-up after 5 years of treatment in patient 1 and after 1.5 years in patient 2, these medications have had no significant effect on bone age advancement. The gonadotrophin-

independent precocious puberty resembles that seen in boys with MAS or testotoxicosis due to activating LHCGR mutations (19).

Other findings
In Patient 1, hypothyroidism was suspected because of a single low fT4 concentration (0.75 ng/ml, reference range: 0.89 – 2.22) with a serum TSH serum concentration in the upper normal range (4.08 mU/l, age related reference range: 0.4 -5.97). Thyroid hormone replacement (25 µg/day) was therefore started at the age of 1 year. In patient 2, TSH concentrations were normal (1.79 mU/l) at 1.2 yrs (age related reference range 0.3-4.0 mU/l).

Patient 2 has two small café-au-lait patches, but neither patient has additional cutaneous features characteristic of MAS and neither had palpable cutaneous ossifications as can be observed in PHP1A. Both patients have delayed motor development and patient 2 also has significantly delayed expressive language. There is no evidence for abnormalities in the GHRH/GH/IGF1 axis, as determined by IGF1 measurements. However, an effect of excessive GH production on growth may have been masked by accelerated bone maturation due to severe precocious puberty [Suppl. Fig. 1].

GNAS nucleotide sequence analyses
Direct nucleotide sequence analysis of *GNAS* exons 1-13 revealed in both patients an identical heterozygous missense *de novo* mutation (c.1126T>G; p.F376V) in exon 13, which was not identified in the parents. Furthermore, whole exome sequencing of patient 1 provided no obvious additional candidate variants explaining the clinical and metabolic phenotype. To determine whether the identified mutation resides on the maternal or the paternal *GNAS* allele, genomic DNA from both patients was amplified across an informative SNP in *GNAS* intron 6 (rs919196) and the c.1126T>G variant; note both patients are C/T, while both mothers are homozygous for C, and both fathers are homozygous for T. Allele separation was performed by cloning the PCR products. Nucleotide sequence analysis of ten independent clones revealed that the *GNAS* exon 13 mutation always segregated together with the maternal cytosine for SNP rs919196, thus documenting that the Gαs mutation resides on the maternal allele.

Functional characterization of Gαs variants
The complex phenotype exhibited by both patients suggested agonist-independent activation of some GPCRs, yet hormonal resistance at others. The Gαs-F376V mutant was therefore functionally assessed in cultured cells by co-expressing wild-type and mutant Gαs with the GPCRs implicated in the different abnormalities, namely V2R (water reabsorption), LHCGR (gonadotrophic action/puberty), PTH1R (mineral ion homeostasis, bone metabolism, and growth plate development), TSHR (thyroid function) or melanocortin-4 receptor (MC4R, weight regulation) [Tab. 2].

To ensure that expression of the G proteins is not influenced by co-transfected receptors, protein levels of wt-Gαs and Gαs-F376V were determined by measurement of luciferase activity in the presence of all tested receptors. Cellular levels of wild-type and mutant Gαs were indistinguishable in the presence of TSHR, V2R, LHCGR and PTH1R; however, in the presence of MC4R, expression of Gαs-F376V was slightly increased [Suppl. Fig. 2]. To gain further insights into how specific side chain properties at position 376 might affect signaling function two additional Gαs variants, p.F376M or p.F376Y were introduced and functionally characterized.

In 2B2 cells, basal cAMP levels were indistinguishable when co-expressing either Gαs-F376V or wt-Gαs with the TSHR or MC4R [Fig. 2A,B]. However, when co-expressed with

V2R, LHCGR, or PTH1R, the Gαs-F376V variant revealed increased basal cAMP accumulation that was 1.6-, 1.5- and 2.3-fold, respectively, higher than that observed with cells co-transfected with wt-Gαs [Fig. 2]. In contrast, agonist-dependent cAMP accumulation was 40-50% lower for all receptors when co-transfected with the F376V mutant, as compared with wt-Gαs [Fig. 2-3]. To validate results obtained in the 2B2 cell system, a second cell system, namely HEK293 cells deficient in Gαs (GSG-5), were used to test the PTH1R in the presence or absence of PTH(1-34) (20). Co-transfection of GSG-5 cells with Gαs-F376V and the PTH1R resulted in approximately 2-fold higher rates of basal cAMP accumulation, as compared to cells co-transfected with wt-Gαs and the PTH1R. However, in comparison to cells expressing wt-Gαs and the PTH1R, the response to PTH(1-34) was blunted in cells co-transfected with Gαs-F376V and the PTH1R [Suppl. Fig. 2].

Additional F376 variants:
Substitution of phenylalanine at position 376 with tyrosine (p.F376Y) resulted in strongly diminished signaling after agonist stimulation when co-expressed with the different GPCRs [Fig. 2-3], which was similar to the findings with the Gαs-F376V mutant. In the absence of agonist, Gαs-F376V revealed similarly enhanced cAMP signaling when coexpressed with V2R, LHCGR and PTH1R [Fig. 2-3]. In contrast, Gαs-F376Y mutant displayed functional properties similar to those of the patient`s mutation leading to the conclusion that the additional hydrophilic hydroxyl-group of the tyrosine modifies the essential hydrophobic core interactions observed with phenylalanine present in wild-type Gαs at this position [Fig. 4].

Surprisingly, the Gαs-F376M substitution revealed more complex signaling properties. For V2R and LHCGR, ligand-induced signaling was comparable to that observed with wild-type Gαs [Fig. 2-3], but was reduced for TSHR [Fig. 2-3]. In contrast, maximal signaling response was enhanced for the PTH1R and the MC4R (1.5- to 2-fold) compared to signaling with wild-type Gαs [Fig. 2-3]. Importantly, methionine at this position does not lead to a significant increase in basal signaling.

Insights from structural homology models
Amino acid F376, located in the C-terminal α5-helix, is highly conserved in the alpha-units of different G proteins [Suppl. Fig. 3]. In the inactive Gαs conformation, the F376 side chain is embedded into a hydrophobic/aromatic cage formed by L43, M60, H64, F212, F219 and M221, located in the β1-, β2-, β3-strands and the N-terminal helix 1 [Fig. 4A1]. These residues rearrange considerably during the activation process to thereby modulate the GDP/GTP-binding pocket. However, unlike disease caused by mutations at residue R201 (9,10), R227 or A366 (12), F376 is not immediately proximal to the nucleotide binding site. Nevertheless, substitution with valine at position 376 (p.F376V) is predicted to disturb the critical network of hydrophobic interactions and to thus indirectly perturb the catalytic site environment [Fig. 4A2]. In contrast, substitution with methionine (p.F376M) largely maintains the essential side chain interactions, which is consistent with the near-normal signaling properties observed for the Gαs-F376M mutant [Fig. 2-3]. The mutation in our patients, Gαs-F376V, with a shorter and more branched side chain compared to phenylalanine, most likely leads to a loss of tight hydrophobic interactions, which then can cause, in comparison to the wild-type protein, modifications in the relative spatial α5-helix orientation. In addition, the p.F376Y mutant with functional properties similar to that of the mutation identified in our patients, strongly supports the conclusion that the additional hydrophilic hydroxyl-group also interrupts the essential hydrophobic core interactions.

Discussion

We here describe a previously unrecognized congenital human disorder caused by a novel, maternal Gαs mutation, namely p.F376V, that is characterized by a unique combination of clinical and laboratory findings, including NSIAD and GnRH-independent precocious puberty. In addition, PTH was elevated because of resistance in the proximal tubules where Gαs is derived predominantly from the maternal *GNAS* allele, thus leading to secondary hyperparathyroidism. However, due to biallelic Gαs expression in most other tissues, including osteoblasts, bone turnover was found to be increased leading to skeletal changes reminiscent of hyperparathyroidism, i.e. changes that can be encountered in PHP1B (21). Furthermore, it appears likely that elevated PTH concentration, combined with normal paternal Gαs expression in chondrocytes, resulted in growth plate changes reminissent of rickets similar to those encountered in a few young patients with PHP1B (22). Irrespective of the underlying mechanisms, the co-incidental identification of two unrelated patients, who presented with indistinguishable, unusual combinations of clinical and metabolic features, strongly suggest that the identified *de novo* p.F376V mutation on the maternal *GNAS* allele accounts for this thus far not described phenotypic profile of the disorder.

A novel feature of both patients was agonist-independent activation of the V2R-regulated pathway leading to NSIAD with the p.F376V mutation in Gαs. Activation of the V2R which is caused by constitutively increased signaling has not been described in MAS nor in any other Gαs-related disease reported to date. The resolution of hyponatremia after early infancy was likely due to adaptive mechanisms, such as changes in nutrition and self-regulation of thirst-driven fluid intake, comparable to that encountered in patients with NSIAD due to gain-of-function mutations in *AVPR2* (23). However, excessive free water intake may in the future again lead to hyponatremia.

Gonadotrophin-independent precocious puberty can be caused by mosaic of Gαs mutated at residue R201, as observed in MAS (10) , or by activating somatic or germline LHCGR mutations (19). In the latter case, the disorder presents with rapid symmetrical growth of testes associated with premature testosterone production. This is clinically similar to the findings in our two patients, but distinct from the frequently, but not always, observed asymmetrical testicular volume encountered with somatic expression of the abnormal Gαs-R201 alleles (24).

Serum PTH concentrations were elevated, yet serum phosphate concentrations were at the upper end of normal or slightly elevated, but not reduced. This is consistent with reduced PTH-responsiveness of the PTH1R/Gαs-F376V complex in the proximal tubule cells where Gαs is expressed predominantly from the maternal *GNAS* allele. As a consequence of increased serum PTH concentrations, augmented PTH1R signaling is predicted to occur when this GPCR is coupled to wt-Gαs derived from the paternal allele, i.e. in tissues with biallelic Gαs expression. The urinary calcium-to-creatinine ratio was low in both patients indicating that calcium reabsorption is fully functional in the distal tubules, where Gαs is expressed from both parental alleles. Thus, either PTH can stimulate efficiently the complex comprising the PTH1R and paternal wt-Gαs, as is observed in PHP1B and PHP1A, and/or ligand-independent calcium reabsorption occurs due to the complex between the PTH1R and the maternal Gαs-F376V mutant.

The skeletal changes leading to bowing of weight-bearing bones as well as the subperiosteal erosions and acro-osteolysis, particularly of the distal phalanges [Fig. 1], were in keeping with enhanced activation of the PTH1R expressed in osteoblasts. These changes might be caused by agonist-independent signaling mediated by complexes formed between the unoccupied PTH1R and Gαs-F376V in osteoblasts which could lead to increased rates of bone turnover and

resorption. However, the agonist-independent effects on osteoblasts, and chondrocytes as outlined above, could be augmented also by elevated serum PTH concentrations and thus sustained activation of the PTH1R coupled to wt-Gαs, which is reminiscent of secondary hyperparathyroidism in children with PHP1B or chronic kidney disease (21,22).

To better understand the mechanisms responsible for this previously unreported human disorder, we co-expressed Gαs variants with a sub-set of GPCRs that are expressed in tissues, which are known to be associated with the symptoms observed in our patients [Tab. 2]. In fact, ligand-independent signaling was induced when the Gαs-F376V mutant was co-expressed with the V2R, PTH1R and LHCGR in concordance with the clinical symptoms of the two patients, but not with the TSHR and MC4R [Fig. 2-3]. Also consistent with *in vivo* evidence for PTH-resistance in proximal tubules our *in vitro* experiments revealed a blunted response to PTH(1-34) when the PTH1R was co-expressed with the Gαs-F376V mutant [Fig. 3 and Suppl. Fig. 3]. The p.F376V mutation resides in both patients on the maternal allele, which contributes in some tissues, such as the proximal renal tubules, most or all Gαs protein. *In vitro,* the response to PTH was blunted at the PTH1R in the presence of the Gαs mutant, which is likely responsible for the PTH elevation caused by PTH1R resistance in this portion of the kidney. It thus appears plausible that the presence of the p.F376V mutation on the paternal *GNAS* allele could lead only to NSIAD and gonadotrophin-independent precocious puberty without PTH resistance. The fact that the maternal p.F376V mutation facilitates ligand-independent cAMP formation in a receptor-specific manner is consistent with the clinical findings observed in both boys. Three different mechanisms are likely to explain the unusual combination of findings in our patients, which include features of both loss- and gain-of-function of Gαs: *(i)* loss-of-function effects that are caused by impaired activity of the Gαs mutant and thus hormonal resistance in those target tissues that rely predominantly or exclusively on maternal Gαs expression, *(ii)* GPCR-dependent gain-of-function effects that are agonist-independent, and *(iii)* effects that are caused by the elevated PTH concentrations and activation of the PTH1R when coupled to the wt-Gαs transcribed from the paternal *GNAS* allele.

At the protein structural level phenylalanine 376 is located near the C-terminus of the Gαs α5-helix and a phenylalanine at this position is highly conserved among all G-protein subtypes [Suppl. Fig. 4]. In the inactive conformation, its aromatic side chain is embedded into a hydrophobic core that is formed by side chains projecting from several different portions of the Gαs scaffold [Fig. 4A1]. This localization enables F376 to act as a key transducer of the conformational forces that propagate from the C-terminal portion of the α5-helix as it engages an activated receptor (25,26) [Fig. 4B] to the interior components of the G-protein that directly participate in the GDP/GTP exchange mechanism (27). A valine mutation at F376 likely causes a marked perturbation of the hydrophobic core configuration and consequently α5-helix changes that differ from those of the wild-type protein [Fig. 4B1]. This hypothesis for Gαs is supported by *in vitro* studies at Gi, where mutations at the corresponding phenylalanine lead to rotation of the α5-helix (28). Moreover, *in vitro* studies at the corresponding phenylalanines of Gαt (29) or Gαi (30) revealed constitutive G-protein activation with respect to an increased GDP/GTP exchange, but they are (partially) resistant to stimulation by agonist-occupied GPCRs. Amino acid F376 in Gαs corresponds to F341 in Gα11 where the p.F341L mutation causes autosomal dominant hypocalcemia (31).

Our experimental data indicate that the p.F376V mutation, combined with the proposed spatial displacement of the α5-helix, decreases ligand-induced down-stream signaling at the investigated receptor/ligand complexes [Fig. 2,3]. As already known from a crystallized

GPCR/Gs complex (16) [Fig. 4B], Gαs undergoes major global and local structural movements during activation (25,27,28,32). This general finding has recently been confirmed at the structural level also for GPCRs complexed with Gi or Go, as elucidated by cryo-electron microscopy (33-35). In the active state, F376 within the GPCR/Gαs complex (16) is located spatially close to the intracellular loop 2 (Il2) of the receptors, but a direct contact was not observed in these GPCR/G-protein complexes without bound nucleotides. Therefore it can only be speculated that F376 may play a crucial role for a potential pre-coupled state, the transition between the inactive and fully-active state, or for dissociation of the G-protein from the GPCRs. In addition, our findings based on side chain variations at position 376 support two hypotheses: *(1)* The receptors are different in their fine-tuned interaction process with Gαs, which would be in accordance with the differences in basal activity observed for the tested GPCRs in complex with the Gαs-F376V mutant. *(2)* Maintenance of the hydrophobic side-chain at this position is essential to facilitate signaling and a methionine can maintain these properties in contrast to a valine.

In summary, the *in vivo* and *in vitro* findings suggest that NSIAD is caused by a recurrent maternal Gαs mutation (p.F376V), which also leads to precocious puberty and skeletal dysplasia [Tab. 2]. It can therefore be expected that other more common diseases, such as precocious puberty or skeletal dysplasia or NSIAD of unknown origin, can be caused by Gαs mutations similar to p.F376V, if these reside on the paternal *GNAS* allele thus enhancing GPCR-independent signaling. The knowledge gained from unique ligand-independent and ligand-dependent consequences caused by this Gαs variant will be helpful in the future development of targeted therapies, and for the clinical management of these patients, for example, restricted fluid intake in view of the predisposition to hyponatremia.

Acknowledgements

Author contributions:

H.B. - designed, conducted and evaluated all functional studies, interpretation of functional data, wrote manuscript, figure preparations; G.K. - design of protein models, wrote the manuscript, interpretation of functional and structural data, contribution to study design, figure preparations; D.S. - initiated clinical studies, clinical data generation; D.B. - initiated clinical studies and manuscript preparation; L.C.W. - clinical phenotype discussions, contributions to manuscript preparation; I.T. - clinical phenotyping, genetic studies; S.K.- clinical phenotyping, contributed to manuscript preparation; P.S. - design of protein models, wrote the manuscript, interpretation of functional and structural data, figure preparations; M.R. - conducted data generation and analysis and interpretation; S.P. - performed functional studies; J.W.G. - initiated clinical studies and clinical data generation and commented on manuscript drafts; J.A. - clinical phenotyping; H.K. - clinical phenotype discussions; M.M. - contributed to the data interpretation and provided insights into experimental models; T.G. - contributed to the data interpretation and provided insights into experimental models; M.D. - designed the clinical and experimental studies, supervised data generation, wrote the manuscript; H.J. - designed the clinical and experimental studies, supervised data generation, interpreted the results and wrote the manuscript; A.G. - designed the clinical and experimental studies, supervised data generation, figure preparations, interpreted the results and wrote the manuscript

§ first authors contributed equally to this work

# last authors contributed equally to this work

*Corresponding author to whom requests should be addressed: Prof. Annette Grüters, Charité-Universitätsmedizin, Department for Pediatric Endocrinology and Diabetes, Mittelallee 8, 13353, Berlin, Germany, Tel.: +49 30 450 566261, email: Annette.Grueters@charite.de

Disclosure statement:
The authors have nothing to disclose.

Abbreviations

AVP, arginine vasopressin; cAMP, cyclic adenosine monophosphate; CG, chorio-gonadotropin; GNAS, G protein alpha subunit; HEK, human embryonic kidney cells; FSH, follitropin; LH, lutropin; LHCGR, lutropin/choriogonadotropin receptor; MAS, McCune-Albright Syndrome; MC4R, Melanocortin-4 receptor; PCR, polymerase chain reaction; PTH, parathyroid hormone; PTH1R, parathyroid hormone receptor; PHP, pseudohypoparathyroidism; V2R, vasopressin-2 receptor; NSIAD, Nephrogenic syndrome of inappropriate anti-diuresis; TSHR, thyroid stimulating hormone receptor; GPCR, G-protein-coupled receptor; TM, transmembrane helix; EL1/2/3, extracellular loops 1/2/3; ILs 1/2/3, intracellular loops 1/2/3; PDB, Protein Data Bank; wt, Wild-type

References

supplementary material is deposited under: Biebermann H. et al., Figshare repository, 30. September 2018. https://figshare.com/s/5954228387e060979a42)

1.   Anantharaman V, Abhiman S, de Souza RF, Aravind L. Comparative genomics uncovers novel structural and functional features of the heterotrimeric GTPase signaling system. Gene 2011; 475:63-78

2.   Oldham WM, Van Eps N, Preininger AM, Hubbell WL, Hamm HE. Mechanism of the receptor-catalyzed activation of heterotrimeric G proteins. Nat Struct Mol Biol 2006; 13:772-777

3.   Limbird LE. The receptor concept: a continuing evolution. Mol Interv 2004; 4:326-336

4.   Farfel Z, Bourne HR, Iiri T. The expanding spectrum of G protein diseases. N Engl J Med 1999; 340:1012-1020

5.   Spiegel AM, Weinstein LS. Inherited diseases involving g proteins and g protein-coupled receptors. Annu Rev Med 2004; 55:27-39

6.   Weinstein LS, Chen M, Xie T, Liu J. Genetic diseases associated with heterotrimeric G proteins. Trends Pharmacol Sci 2006; 27:260-266

7.   Hu Q, Shokat KM. Disease-Causing Mutations in the G Protein Galphas Subvert the Roles of GDP and GTP. Cell 2018;

8.   O'Hayre M, Vazquez-Prado J, Kufareva I, Stawiski EW, Handel TM, Seshagiri S, Gutkind JS. The emerging mutational landscape of G proteins and G-protein-coupled receptors in cancer. Nat Rev Cancer 2013; 13:412-424

9.   Riminucci M, Fisher LW, Majolagbe A, Corsi A, Lala R, De Sanctis C, Robey PG, Bianco P. A novel GNAS1 mutation, R201G, in McCune-albright syndrome. J Bone Miner Res 1999; 14:1987-1989

10.   Weinstein LS, Shenker A, Gejman PV, Merino MJ, Friedman E, Spiegel AM. Activating mutations of the stimulatory G protein in the McCune-Albright syndrome. N Engl J Med 1991; 325:1688-1695

11.   Aldred MA, Trembath RC. Activating and inactivating mutations in the human GNAS1 gene. Hum Mutat 2000; 16:183-189

12.   Iiri T, Herzmark P, Nakamoto JM, van Dop C, Bourne HR. Rapid GDP release from Gs alpha in patients with gain and loss of endocrine function. Nature 1994; 371:164-168

13.   Tarnow P, Schoneberg T, Krude H, Gruters A, Biebermann H. Mutationally induced disulfide bond formation within the third extracellular loop causes melanocortin 4 receptor inactivation in patients with obesity. J Biol Chem 2003; 278:48666-48673

14.   Bastepe M, Gunes Y, Perez-Villamil B, Hunzelman J, Weinstein LS, Juppner H. Receptor-mediated adenylyl cyclase activation through XLalpha(s), the extra-large variant of the stimulatory G protein alpha-subunit. Mol Endocrinol 2002; 16:1912-1919

15.   Winkler F, Kleinau G, Tarnow P, Rediger A, Grohmann L, Gaetjens I, Krause G, L'Allemand D, Gruters A, Krude H, Biebermann H. A new phenotype of nongoitrous and nonautoimmune hyperthyroidism caused by a heterozygous thyrotropin receptor mutation in transmembrane helix 6. J Clin Endocrinol Metab 2010; 95:3605-3610

16.   Rasmussen SG, DeVree BT, Zou Y, Kruse AC, Chung KY, Kobilka TS, Thian FS, Chae PS, Pardon E, Calinski D, Mathiesen JM, Shah ST, Lyons JA, Caffrey M, Gellman SH, Steyaert J, Skiniotis G, Weis WI, Sunahara RK, Kobilka BK. Crystal structure of the beta2 adrenergic receptor-Gs protein complex. Nature 2011; 477:549-555

17.   Sunahara RK, Tesmer JJ, Gilman AG, Sprang SR. Crystal structure of the adenylyl cyclase activator Gsalpha. Science 1997; 278:1943-1947

18.   Wall MA, Coleman DE, Lee E, Iniguez-Lluhi JA, Posner BA, Gilman AG, Sprang SR. The structure of the G protein heterotrimer Gi alpha 1 beta 1 gamma 2. Cell 1995; 83:1047-1058

19.   Shenker A, Laue L, Kosugi S, Merendino JJ, Jr., Minegishi T, Cutler GB, Jr. A constitutively activating mutation of the luteinizing hormone receptor in familial male precocious puberty. Nature 1993; 365:652-654

20.   Milligan G, Inoue A. Genome Editing Provides New Insights into Receptor-Controlled Signalling Pathways. Trends Pharmacol Sci 2018; 39:481-493

21.   Farfel Z. Pseudohypohyperparathyroidism-pseudohypoparathyroidism type Ib. J Bone Miner Res 1999; 14:1016

22.   Grigelioniene G, Nevalainen PI, Reyes M, Thiele S, Tafaj O, Molinaro A, Takatani R, Ala-Houhala M, Nilsson D, Eisfeldt J, Lindstrand A, Kottler ML, Makitie O, Juppner H. A Large

Inversion Involving GNAS Exon A/B and All Exons Encoding Gsalpha Is Associated With Autosomal Dominant Pseudohypoparathyroidism Type Ib (PHP1B). J Bone Miner Res 2017; 32:776-783

23.   Bockenhauer D, Penney MD, Hampton D, van't Hoff W, Gullett A, Sailesh S, Bichet DG. A family with hyponatremia and the nephrogenic syndrome of inappropriate antidiuresis. Am J Kidney Dis 2012; 59:566-568

24.   Boyce AM, Chong WH, Shawker TH, Pinto PA, Linehan WM, Bhattacharryya N, Merino MJ, Singer FR, Collins MT. Characterization and management of testicular pathology in McCune-Albright syndrome. J Clin Endocrinol Metab 2012; 97:E1782-1790

25.   Scheerer P, Heck M, Goede A, Park JH, Choe HW, Ernst OP, Hofmann KP, Hildebrand PW. Structural and kinetic modeling of an activating helix switch in the rhodopsin-transducin interface. Proc Natl Acad Sci U S A 2009; 106:10660-10665

26.   Scheerer P, Park JH, Hildebrand PW, Kim YJ, Krauss N, Choe HW, Hofmann KP, Ernst OP. Crystal structure of opsin in its G-protein-interacting conformation. Nature 2008; 455:497-502

27.   Chung KY, Rasmussen SG, Liu T, Li S, DeVree BT, Chae PS, Calinski D, Kobilka BK, Woods VL, Jr., Sunahara RK. Conformational changes in the G protein Gs induced by the beta2 adrenergic receptor. Nature 2011; 477:611-615

28.   Alexander NS, Preininger AM, Kaya AI, Stein RA, Hamm HE, Meiler J. Energetic analysis of the rhodopsin-G-protein complex links the alpha5 helix to GDP release. Nat Struct Mol Biol 2014; 21:56-63

29.   Kapoor N, Menon ST, Chauhan R, Sachdev P, Sakmar TP. Structural evidence for a sequential release mechanism for activation of heterotrimeric G proteins. J Mol Biol 2009; 393:882-897

30.   Kaya AI, Lokits AD, Gilbert JA, Iverson TM, Meiler J, Hamm HE. A conserved phenylalanine as a relay between the alpha5 helix and the GDP binding region of heterotrimeric Gi protein alpha subunit. J Biol Chem 2014; 289:24475-24487

31.   Nesbit MA, Hannan FM, Howles SA, Babinsky VN, Head RA, Cranston T, Rust N, Hobbs MR, Heath H, 3rd, Thakker RV. Mutations affecting G-protein subunit alpha11 in hypercalcemia and hypocalcemia. N Engl J Med 2013; 368:2476-2486

32.   Dror RO, Mildorf TJ, Hilger D, Manglik A, Borhani DW, Arlow DH, Philippsen A, Villanueva N, Yang Z, Lerch MT, Hubbell WL, Kobilka BK, Sunahara RK, Shaw DE. SIGNAL TRANSDUCTION. Structural basis for nucleotide exchange in heterotrimeric G proteins. Science 2015; 348:1361-1365

33.   Draper-Joyce CJ, Khoshouei M, Thal DM, Liang YL, Nguyen ATN, Furness SGB, Venugopal H, Baltos JA, Plitzko JM, Danev R, Baumeister W, May LT, Wootten D, Sexton PM, Glukhova A, Christopoulos A. Structure of the adenosine-bound human adenosine A1 receptor-Gi complex. Nature 2018; 558:559-563

34.   Garcia-Nafria J, Nehme R, Edwards PC, Tate CG. Cryo-EM structure of the serotonin 5-HT1B receptor coupled to heterotrimeric Go. Nature 2018; 558:620-623

35.   Koehl A, Hu H, Maeda S, Zhang Y, Qu Q, Paggi JM, Latorraca NR, Hilger D, Dawson R, Matile H, Schertler GFX, Granier S, Weis WI, Dror RO, Manglik A, Skiniotis G, Kobilka BK. Structure of the micro-opioid receptor-Gi protein complex. Nature 2018; 558:547-552

Figure 1: *Radiographic studies of skeletal features in the patients.* Radiographs of patient 1 showing the skeletal abnormalities such as antecurvatura of the left distal tibia, bowing of both

upper legs, enlargement of the metaphyses. **A)** Radiographic study of patient 1, at 1 year 8 months and 7 years. **B)** Radiographic study of patient 2 at 1 year and 3 months.

Figure 2: *Functional characterization of wt Gαs and variants co-expressed with several different GPCRs.* 2B2 cells were co-transfected with GPCRs, and either wild-type or mutant Gαs, as indicated. After two days, cAMP accumulation was determined in the absence or presence of maximal concentration of indicated ligands by alpha screen technology. Results of four independent experiments performed in triplicated were shown as mean ± SEM. Statistical analysis was performed with one-way ANOVA with Kruskal-Wallis test, indicated receptors + Gαs were tested against receptors in the presence of different Gαs variants; * $p \leq 0.05$, ** $p \leq 0.01$, ***$p \leq 0.001$, ****$p \leq 0.0001$.

Figure 3: *Functional characterization of wt Gαs and variants co-expressed with different GPCRs.* 2B2 cells were co-transfected with GPCRs, and wild-type or mutant Gαs, as indicated. After two days, cAMP accumulation was determined in the presence of decadic increasing concentration of indicated ligands by alpha screen technology. Results of four independent experiments performed in triplicates were shown as mean ± SEM.

Figure 4: *Phenylalanine 376 in different Gαs conformations and activity states.* **A-A1)** In the inactive state conformation of the heterotrimeric Gαs amino acid F376 is cage-like embedded by several hydrophobic and/or aromatic amino acids (shown as green sticks). F376 is not directly located at the GDP/GTP (shown as orange spheres) binding pocket unlike known pathogenic Gαs mutations, *e.g.* residues A366, R201 or Q227 (7) (magenta sticks). **A2).** Mutational variants such as p.F376V, p.F376Y and p.F376M lead to specific changes in the tight hydrophobic/aromatic environment at position 376. Methionine is aliphatic in contrast to phenylalanine, but is hydrophobic and interacts with aromatic ring systems. Valine is characterized by a shorter and more branched side chain compared to phenylalanine. The patient mutant F376V therefore most likely leads to a loss of the tight interactions, which finally can cause structural modifications in the relative spatial α5-helix orientation compared to wild-type. **B)** From the crystal structure Gαs/β-2AR complex (PDB entry 3SN6 (16)) it is known that the Gαs-protein undergoes structural re-organization during interaction with the receptor, *e.g.* a global movement of the helical domain (arrow), enabled by ligand-induced conformational changes in the receptor. **B1)** The superimposition between the active and the inactive Gs crystal structure shows that F376 changes the spatial localization during G-protein activation related to local movements of the C-terminal α5-helix.

Table 1: *Clinical and metabolic findings in the two patients.* Clinical and biochemical findings in the patients with p.F376V compared to patients with pseudohypoparathyroidism and precocious puberty (p.A366S) caused by protein instability (12) or found in McCune Albright Syndrome (p.R201H) (10). Characteristic findings of the three different diseases are highlighted. "+" present, "-" not present, "+/- " unilateral testes enlargement

	Patient 1 this study	Patient 2 this study	Precocious puberty and PTH resistance	McCune Albright Syndrome
	F376V germline	**F376V germline**	**A366S germline**	**R201H postzygotic**
Serum sodium (mmol/l, normal range 129 – 145)	117- 123	118-142	not reported	normal
Serum PTH (pg/ml, normal range 15-57)	66 – 454	90-215	570	normal

Serum alkaline phosphatase (U/l, normal range:125-380)	350 – 853	217-262	550 – 830	normal
Serum calcium (mmol/l, normal range 2.2-2.6))	2.4 – 2.8	2.16-2.4	1.4 -2.2	normal
Serum phosphate (mmol/l, normal range 1.1 -2.15)	1.4 -1.8	1.75-2.15	2.0 - 3.1	normal
Serum Testosterone (at 3 - 6 years) (ng/ml, normal range 10-65)	510 – 990	314 - 609	47 - 692	normal or elevated
LH (U/L) (30 min after GnRH)	< 0.1	< 0.1	< 1	< 0.1
FSH (U/L) (30 min after GnRH)	< 0.1	< 0.1	< 2	< 0,1
Enlarged testes	+	+	+	+/-
Serum fT4 (ng/L, normal range 9.6 -17.7) or T4 (µg/dl, 5.0 -12.0)	8.4	11-13	3.1 -6.9 (T4)	normal or high-
Serum TSH (mU/L, normal range 0.7 – 5.9)	0.6 - 4.1	2-2.3	1 - 2.6 mU/l	normal or suppressed
Copeptin (pmol/L)	n.d.	2.4-3.6	not reported	not reported
Plasma Osmolality (mOsm/kg)	241 - 271	282-290	not reported	not reported
Urine Osmolality (mOsm/kg)	n.d.	769-1006	not reported	not reported
BMI (SDS) at 3 years	+ 3.21	+ 3.89	weight > 95th percentile	normal weight-
Osteopenia	-	-	+	not reported
Brachydactyly	-	-	+	-
Resorptive osteolytic cysts	-	-	+	+
Café au lait spots	-	(+)	-	+

Table 2: *Review of inherited human diseases caused by impaired GPCR function.* Human diseases caused by variants of GPCR or Gαs of either loss- or gain-of-function consequences including the novel phenotypes caused by variant **p.**F376V studied in this report. Receptor +/Gαs + = gain-of-function variants, Receptor -/Receptor - = Loss-of-function variants

Spalte1	Receptor - Phenotypes	Receptor + Phenotypes	Gs - Phenotypes	Gs + Phenotypes
	loss-of-function mutation	gain-of-function mutation	loss-of-function mutation/maternal imprinting	gain-of-function mutation +
LHCGR	Leydig cell hypoplasia (male)	precocious puberty (male)	unknown	precocious puberty (Mc Cune Albright), male + female
	hypergonadotrophic hypogonadism (male and female)	Leydig cell adenoma (male)		
TSHR	congenital hypothyroidism	non-autoimmune hyperthyroidism	hyperthryotropinemia	hyperthyroidism (Mc Cune Albright)
	hyperthyrotropinemia	thyroid adenoma	hypothyroidism	thyroid adenoma
PTH1R	Bloomstrand chondrodysplasia	Jansen metaphyseal chondrodysplasia	Albright Herediatry osteodystrophy	**new: this report (F376V)**
			Pseudohypoparathyroidism	**Fibrous dysplasia (Mc Cune Albright)**
V2R	X-linked nephrogenic diabetes insipidus	NSIAD	unknown	**new: NSIAD this report (F376V)**

Patient 1

1 year 8 months
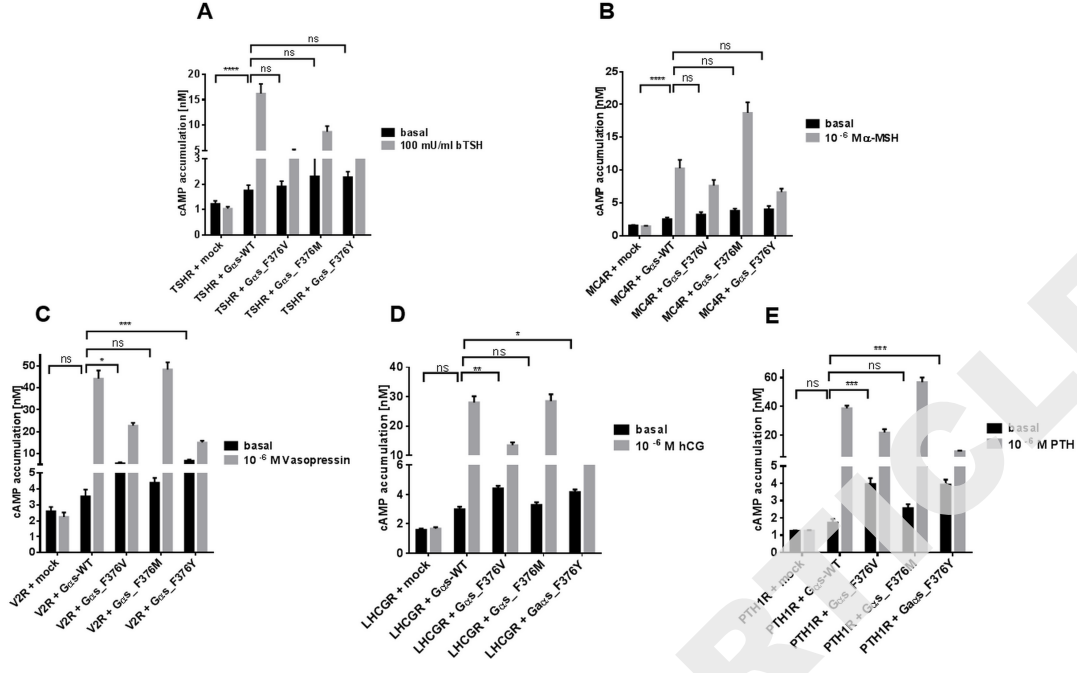

7 year 6 months

Patient 2

1 year 3 months

A

TSHR + mock
TSHR + Gαs-WT
TSHR + Gαs_F376V
TSHR + Gαs_F376M
TSHR + Gαs_F376Y

cAMP accumulation [nM]

log bTSH [mU/ml]

B

MC4R + mock
MC4R + Gαs-WT
MC4R + Gαs_F376V
MC4R + Gαs_F376M
MC4R + Gαs_F376Y

cAMP accumulation [nM]

log α-MSH [M]

C

V2R + mock
V2R + Gαs-WT
V2R + Gαs_F376V
V2R + Gαs_F376M
V2R + Gαs_F376Y

cAMP accumulation [nM]

log Vasopressin [nM]

D

LHCGR + mock
LHCGR + Gαs-WT
LHCGR + Gαs_F376V
LHCGR + Gαs_F376M
LHCGR + Gαs_F376Y

cAMP accumulation [nM]

log hCG [M]

E

PTH1R + mock
PTH1R + Gαs-WT
PTH1R + Gαs_F376V
PTH1R + Gαs_F376M
PTH1R + Gαs_F376Y

cAMP accumulation [nM]

log hPTH [M]